Journal of Applied Polymer Science

Mechanical and thermal properties of SEBS-g-MA compatibilized halloysite nanotubes reinforced polyethylene terephthalate/polycarbonate/nanocomposites

Nurul Ain Jamaludin,[1] Ibrahim Mohammad Inuwa,[1] Azman Hassan,[1] Norhayani Othman,[1] Mohammed Jawaid[2]

[1]Faculty of Chemical Engineering, Department of Polymer Engineering, Universiti Teknologi Malaysia, Skudai, Johor, Malaysia
[2]Laboratory of Biocomposite Technology, Institute of Tropical Forestry and Forest Products (INTROP), Universiti Putra Malaysia, Selangor, Malaysia
Correspondence to: A. Hassan (E-mail: azmanh@cheme.utm.my)

ABSTRACT: In this study, the effect of maleic anhydride grafted styrene-ethylene-butylene-styrene (SEBS-*g*-MA) content on mechanical, thermal, and morphological properties of polyethylene terephthalate/polycarbonate/halloysite nanotubes (PET/PC/HNTs) nanocomposites has been investigated. Nanocomposites of PET/PC (70 : 30) with 2 phr of HNTs were compounded using the counter rotating twin screw extruder. A series of formulations were prepared by adding 5–20 phr SEBS-*g*-MA to the composites. Incorporation of 5 phr SEBS-*g*-MA into the nanocomposites resulted in the highest tensile and flexural strength. Maximum improvement in the impact strength which is 245% was achieved at 10 phr SEBS-*g*-MA content. The elongation at break increased proportionately with the SEBS-*g*-MA content. However, the tensile and flexural moduli decreased with increasing SEBS-*g*-MA content. Scanning electron microscopy revealed a transition from a brittle fracture to ductile fracture morphology with increasing amount of SEBS-*g*-MA. Transmission electron microscopy showed that the addition of SEBS-*g*-MA into the nanocomposites promoted a better dispersion of HNTs in the matrix. A single glass transition temperature was observed from the differential scanning calorimetry test for compatibilized nanocomposites. Thermogravimetric analysis of PET/PC/HNTs nanocomposites showed high thermal stability at 15 phr SEBS-*g*-MA content. However, on further addition of SEBS-*g*-MA up to 20 phr, thermal stability of the nanocomposites decreased due to the excess amount of SEBS-*g*-MA. © 2015 Wiley Periodicals, Inc. J. Appl. Polym. Sci. **2015**, *132*, 42608.

KEYWORDS: blends; compatibilization; composites; mechanical properties; thermal properties

Received 27 January 2015; accepted 7 June 2015
DOI: 10.1002/app.42608

INTRODUCTION

Polyethylene terephthalate (PET) is a thermoplastic polymer of the polyester family. Depending on its processing and thermal history, PET may exist both as an amorphous and as semi crystalline.[1] Because of its high performance, low cost, and recyclability, it has become the most important member of the polyester thermoplastics.[2] Besides blow molded bottles, it is also used as extruded films, sheets, monofilaments, and also for textile fibers.[3] Properties such as strength, stiffness, chemical resistance, transparency, and thermal stability of PET are the basis for its broad application. Despite these advantages, PET has shortcoming of poor impact strength, high moisture absorption and slow crystallization rate which limits its use in certain applications. For example, PET containers shrink or distort above 80°C. Some of the measures taken to eliminate these shortcomings are by blending with other polymers or reinforcements with fillers to form composites. Polycarbonate (PC) is an engineering thermoplastic with excellent properties such as stiffness, high impact strength, high heat deflection temperature, and high glass transition temperature. As a result it is widely used as commercial thermoplastics for engineering applications. However, PC is characterized by poor solvent resistance which limits its applications in chemical environment. PET/PC blend offer a convenient solution for the poor solvent resistance of PC and the poor impact properties of PET. However, blending of PET and PC has reduced some of the useful properties of PC such as stiffness, impact strength and heat deflection temperature due to limited miscibility.[4–7] To compensate for the loss of these properties a suitable reinforcement may need to be incorporated to develop composite materials with good properties.

Halloysite nanotubes (HNTs) are eco-friendly nanotubes with low cost compared to carbon nanotubes. HNTs are widely used

as additives in polymers, for electric components, drug delivery systems, cosmetics and for personal care products applications.[8] Du *et al.*[9] have studied the thermal stability and flame retardant effects of HNTs in polypropylene (PP) based composites. They found that HNTs are effective for improving the thermal stability and flame retardancy of PP and can be easily processed. Another study conducted by Höchstötter *et al.*[10] on polyamide-6 (PA6) based nanocomposites revealed that the tensile strength, tensile modulus and elongation at break was improved at low HNTs content. They observed that the incorporation of 2 wt % of HNTs increased the mechanical properties. However, the mechanical properties decreased at 5 wt % HNTs content due to the formation of agglomerates confirmed by SEM. HNTs filled thermoplastics nanocomposites have been widely studied, however, the study on incorporating HNTs in PET/PC blends has not been reported in the literature. In the development of PET/PC/HNTs nanocomposites, one of the most important aspects is to achieve good combination of properties. Mubarak[11] investigated PET/PC nanocomposites using nanodispersed organically modified layered silicates (Nanofil 9) as reinforcements. The samples became very brittle as the percentage of the Nanofil 9 increased due to the poor dispersion of nanoparticles within the blends. Some of the factors that limit the potential of polymer nanocomposites are the compatibility, interfacial adhesion between the phases, dispersion of clay in polymer matrix and ductility/toughness of the nanocomposites.[12]

The addition of HNTs into PET/PC blends have improved the stiffness and strength of the resulting nanocomposites, however, the impact properties of the synthesized nanocomposites have deteriorated even at low concentration due agglomeration of the nanofillers and lack of interfacial adhesion. Therefore, an impact modifier is needed to balance the stiffness, strength, and impact properties of the nanocomposites.

Maleic anhydride grafted styrene-ethylene-butylene-styrene (SEBS-*g*-MA) was incorporated to serve as impact modifier as well as compatibilizer to improve the adhesion between matrix and filler and to compatibilize the PET/PC blend. Lim and Chow[13] investigated the use of SEBS-*g*-MA in PET/organo-montmorillonite (OMMT) nanocomposites. The impact strength of PET was reduced by the addition of OMMT due to the embrittlement effect of the clay. Addition of 5 wt % of SEBS-*g*-MA increased the impact strength and stabilized the morphology of PET/OMMT nanocomposites. The presence of maleic anhydride functionalized SEBS act as emulsifier to decrease the interfacial tension by improved adhesion between the phases and promoted better dispersion of the elastomer in the melt.[14] It has been well established that the reaction between the anhydride group of the SEBS-*g*-MA and the PET ester group or terminal –OH group resulted in strong adhesion of PET and SEBS phases.[14,15]

Although several polymer systems have been reinforced with HNTs no report is available on the use of HNTs to reinforce PET/PC blend matrix modified with SEBS-*g*-MA impact modifiers. The objective of this work was to evaluate the effect of SEBS-*g*-MA on the mechanical and thermal properties of 70PET/30PC/2HNTs nanocomposites. Melt extrusion is the most attractive method for the dispersion of nanofillers in polymeric matrices due to its simplicity and adaptability with the current industrial machineries.

Table I. Composition of the PET/PC Nanocomposites

Sample name	PET (wt %)	PC (wt %)	HNT (phr)	SEBS-*g*-MA (phr)
SEBS0	70	30	2	0
SEBS5	70	30	2	5
SEBS10	70	30	2	10
SEBS15	70	30	2	15
SEBS20	70	30	2	20

EXPERIMENTAL

Materials

PET (EM 100) used was supplied by Recron Malaysia Sdn. Bhd. It has an intrinsic viscosity of 0.78–0.84 dL/g, melting temperature of 245–255°C (DSC, ASTM E 928) and molecular weight of about 30,000 g/mole. PC, Panlite L-1225Y grade, was supplied by Teijin Chemical, melt flow index at 300°C of 11.0 cm^3/10 min and density of 1.20 g/cm^3. The HNT (Dragonite) was obtained from Applied Minerals, New York. The elemental composition of HNTs is as follows (wt %): $Al_2O_3.2SiO_2.2H_2O$, 95; SiO_2.[5] The specific gravity is 2.53. SEBS-*g*-MA was supplied by Shell Chemical Co. under the trade name of Kraton FG 1901X.

Melt Processing

PET and PC pellets were dried for more than 8 h at 110°C in oven. A detailed formulation of the prepared nanocomposites is shown in Table I. PET, PC, HNT, and SEBS-*g*-MA were manually premixed in a container then fed into the hopper of a counter-rotating twin screw extruder Plastic Corder, PL 2000. The extruder temperatures were set at 220°C (zone 1), 240°C (zone 2), 245°C (zone 3), and 250°C (die). The screw speed was set at 60 rpm. The extruded products were cooled and cut into pellet form using laboratory scale pelletizer. The pellets were dried at 110°C for 12 h before injection molding using an injection molding machine (JSW 100 Ton) made in Japan. The temperatures from the hopper to the nozzle were in the range of 220–250°C.

Mechanical Properties

Flexural and tensile properties of the nanocomposites samples were determined using Lloyd universal testing machine according to ASTM D790-07 and ASTM D638, respectively. For flexural and tensile measurements, crosshead speed of 3 mm/min and 30 mm/min were used, respectively. Notched Izod Impact test (ASTM D256) was performed using Izod Toyoseiki (11 joule) impact tester. All tests were conducted under ambient conditions. Ten specimens were measured and the average value was recorded.

Differential Scanning Calorimetry

Differential Scanning Calorimetry (DSC) was conducted at the heating rate of 10°C/min and at temperature ranging from 25°C to 500°C, using sample size approximately 10 mg in accordance with ASTM D3418-82 testing procedures.

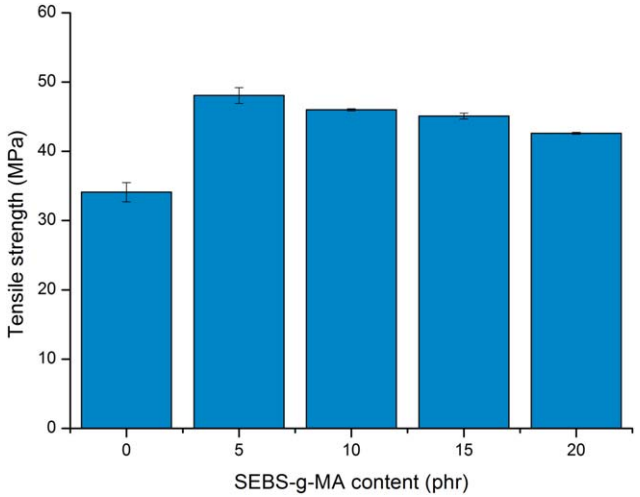

Figure 1. Effect of SEBS-*g*-MA content on tensile strength of PET/PC nanocomposites. [Color figure can be viewed in the online issue, which is available at wileyonlinelibrary.com.]

Thermogravimetric Analysis

Thermal stability of the nanocomposites was measured using a thermogravimetric analyzer (Perkin Elmer TGA7) at 10°C/min under a nitrogen atmosphere from 30 to 650°C.

Scanning Electron Microscopy

The surface morphologies of tensile fractured specimens were observed via scanning electron microscope (SEM, Philips XL40). The samples were coated with a thin layer of gold before the observations.

Transmission Electron Microscopy

The phase structure or pattern of dispersion in the nanocomposites was studied using transmission electron microscopy (TEM), Philips TEM CM12. The specimens were prepared using Leica Ultracut UCT ultra microtome. Ultra-thin sections of about 60 nm in thickness were cut with a diamond knife at room temperature (35°C).

Fourier Transforms Infrared Spectroscopy

To study the interaction between the nanocomposites, Fourier transforms infrared (FTIR) was performed using a Perkin Elmer 1600 Infrared spectrometer. FTIR spectra of the samples were recorded using Nicolet's AVATAR 360 at 32 scans with a resolution of 4 cm^{-1} in the range of 4000–500 cm^{-1}.

RESULTS AND DISCUSSION

Mechanical Properties

Tensile Properties. Figure 1 shows the effect of SEBS-*g*-MA content on tensile strength of 70PET/30PC/2HNTs nanocomposites. Generally the tensile strength of SEBS-*g*-MA compatibilized formulations are higher than the uncompatibilized nanocomposites. The maximum increase of 41% was achieved upon the addition of 5 phr of SEBS-*g*-MA. However, at 10 phr and higher SEBS-*g*-MA content, a decrease in tensile strength was observed. These enhancements is attributed to the good interfacial adhesion between the filler and the matrix due to the addition of SEBS-*g*-MA. The improved interfacial adhesion between the matrices results from reaction of maleic anhydride of SEBS-*g*-MA with the hydroxyl end group of PET and PC[16] and a possible interaction between the maleic anhydride and hydroxyl groups on the outer wall of HNTs.

These results are in agreement with the findings of Kusmono *et al.*[17] on the effect of SEBS-*g*-MA on mechanical properties of PA6/PP/OMMT nanocomposites. They reported that the tensile strength of nanocomposites increased in the presence of SEBS-*g*-MA. The miscibillity of SEBS-*g*-MA with polar groups of the nanoparticles and the matrix contributes to the increment in the tensile strength. The tensile strength started to decrease with high content of SEBS-*g*-MA. Studies by Zhang *et al.*[18] showed that the tensile strength of recycled PET decreased with higher SEBS-*g*-MA loading due to elastomeric nature of unreacted SEBS-*g*-MA.

The effect of SEBS-*g*-MA content on tensile modulus of 70PET/30PC/2HNTs nanocomposites is shown in Figure 2. Progressive decrease in the tensile modulus was observed with increasing of SEBS-*g*-MA content. The addition of 5 phr SEBS-*g*-MA resulted in a 6.7% initial reduction in tensile modulus of 70PET/30PC/2HNTs nanocomposites. Similar observation was reported by Tjong and Bao[19] on effect of SEBS-*g*-MA on tensile modulus of PA6/clay nanocomposites. They found that reduction in stiffness of PA6/clay nanocomposites attributed to the elastomeric nature of SEBS-*g*-MA.

Figure 3 shows the effect of SEBS-*g*-MA content on elongation at break of 70PET/30PC/2HNTs nanocomposites. The addition of 5 phr of SEBS-*g*-MA increased the elongation at break by about 109% compared to SEBS0 nanocomposites. It can be seen that all the SEBS-*g*-MA toughened PET/PC nanocomposites exhibited higher elongation at break compared to SEBS0 nanocomposites. Similar results were found by Chow and Neoh[20]on their study of mechanical properties of PC/SEBS-*g*-MA/montmorillonite nanocomposites. Elongation at break increased with increasing the SEBS-*g*-MA contents. They mentioned that the enhancement of elongation at break was due to the ability of the elastomer structure in SEBS-*g*-MA to absorb and dissipate

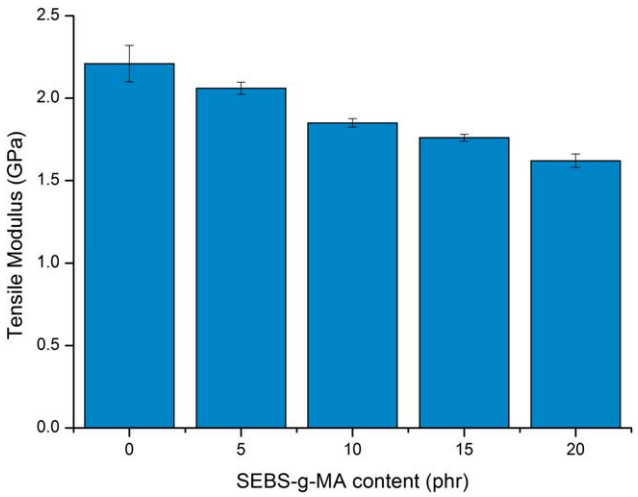

Figure 2. Effect of SEBS-*g*-MA content on tensile modulus of PET/PC nanocomposites. [Color figure can be viewed in the online issue, which is available at wileyonlinelibrary.com.]

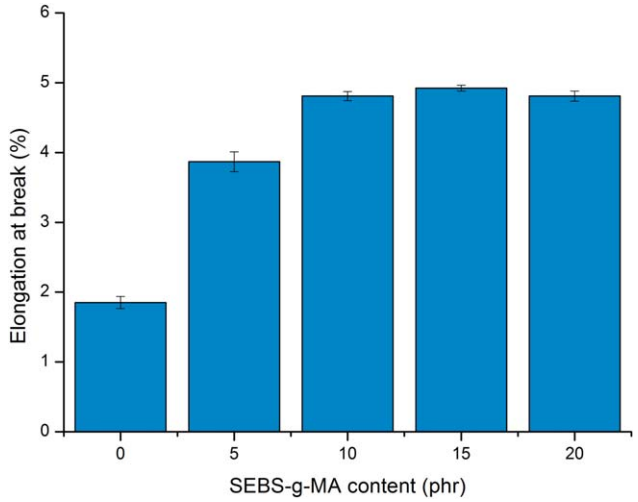

Figure 3. Effect of SEBS-*g*-MA content on elongation at break of PET/PC nanocomposites. [Color figure can be viewed in the online issue, which is available at wileyonlinelibrary.com.]

the energy upon applied external force. According to Kusmono *et al.*[17] the elastomeric nature of SEBS-*g*-MA acts as stress concentrator around the nanofiller particles during strain process during tensile testing.

Flexural Properties. The effect of SEBS-*g*-MA content on flexural strength of 70PET/30PC/2HNTs nanocomposites is shown in Figure 4. It can be seen that, the addition of SEBS-*g*-MA increased the flexural strength of the 70PET/30PC/2HNTs nanocomposites. The highest flexural strength value was at 5 phr of SEBS-*g*-MA content and then decreased with increasing SEBS-*g*-MA content. This trend resembles to that of the tensile strength. The increment in the flexural strength was attributed to the good interfacial adhesion between the phases. The maleic anhydride functional group of SEBS-*g*-MA reacts with hydroxyl end group of PET and PC, which attribute to strengthen interfacial adhesion and improve the compatibility between components as

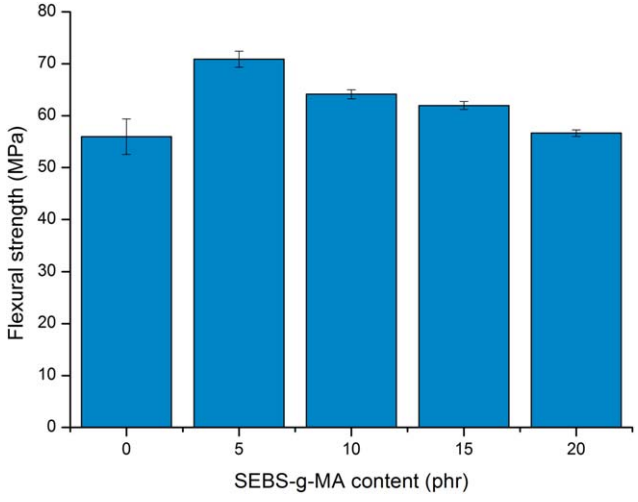

Figure 4. Effect of SEBS-*g*-MA content on flexural strength of PET/PC nanocomposites. [Color figure can be viewed in the online issue, which is available at wileyonlinelibrary.com.]

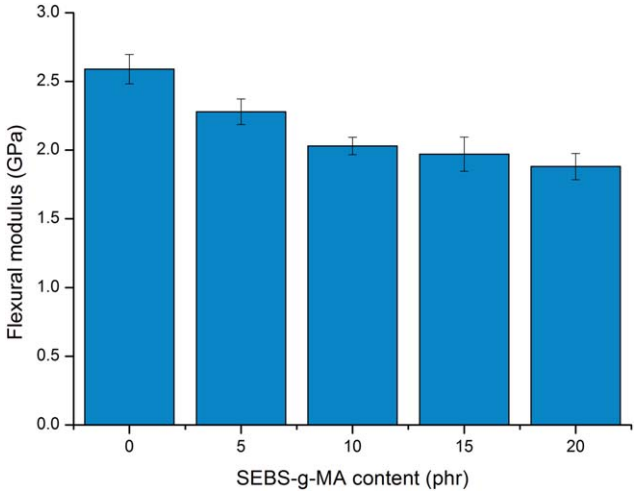

Figure 5. Effect of SEBS-*g*-MA contents on flexural modulus of PET/PC nanocomposites. [Color figure can be viewed in the online issue, which is available at wileyonlinelibrary.com.]

reported by Tang *et al.*[16] The decrease in the flexural strength at higher SEBS loading can be related to elastomeric nature of the excess SEBS-*g*-MA. Similar finding was reported by Heino *et al.*[21] on compatibility of PET/PP with SEBS-*g*-MA. They reported that the flexural strength was lowered as expected due to elastic behavior of the compatibilizer.

Figure 5 display the effect of SEBS-*g*-MA content on flexural modulus of 70PET/30PC/2HNTs nanocomposites. It can be seen that the addition of SEBS-*g*-MA into 70PET/30PC/2HNTs nanocomposites resulted in a decrease in its flexural modulus value. A similar trend to the tensile modulus was observed. The reduction in flexural modulus is attributed to the low modulus elastomeric phase of SEBS-*g*-MA. Similar observation was reported by Kusmono *et al.*[22] on influence of SEBS-*g*-MA on mechanical properties of PA6/PP/organoclay nanocomposites. They reported that the flexural modulus was reduced with the incorporation of SEBS-*g*-MA. They found that the reduction in flexural modulus was attributed to the elastomeric characteristic of the SEBS-*g*-MA.

Impact Strength. The effect of SEBS-*g*-MA content on the impact strength of 70PET/30PC/2HNTs nanocomposites is shown in Figure 6. Interestingly, the impact strength significantly increased with increasing SEBS-*g*-MA contents. The elastomeric nature of SEBS and the presence of MA in SEBS acted as an emulsifier to decrease the interfacial tension. More energy was able to be absorbed due the toughening effect of SEBS-*g*-MA. Hence, the impact strength increased. It is interesting to note that the incorporation of 10 phr SEBS-*g*-MA to nanocomposites led to significant improvement in the impact strength up to 245%. This improvement reflects the ability of SEBS-*g*-MA to act as impact modifier for the PET/PC/HNT system. Tjong and Bao[19] had reported similar observation where the addition of SEBS-*g*-MA had increased the impact strength of PA6 nanocomposites. The total fracture energy is completely dissipated in the inner region near the fracture surface, and no energy is dissipated in the outer plastic zone. The presence of

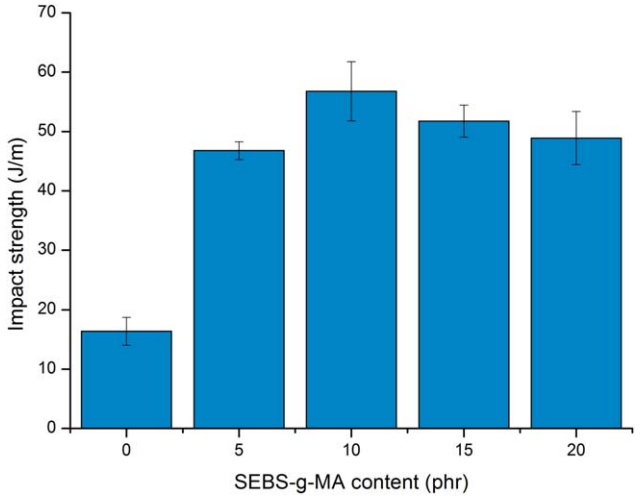

Figure 6. Effect of SEBS-*g*-MA content on impact strength of PET/PC nanocomposites. [Color figure can be viewed in the online issue, which is available at wileyonlinelibrary.com.]

SEBS-*g*-MA enhances the energy of crack propagation during the impact loading. However, the impact strength decreased as the content of SEBS-*g*-MA more than 15 phr due to the presence of excess unreacted SEBS-*g*-MA. Chow and Neoh[20] observed a decrease in impact strength of SEBS-*g*-MA toughened PC/MMT nanocomposites. They reported that the impact strength is reduced when the amount of SEBS-*g*-MA exceeded the optimum loading.

Differential Scanning Calorimetry. Figures 7 and 8 show the DSC heating and cooling thermograms of 70PET/30PC/2HNTs nanocomposites with and without SEBS-*g*-MA. The melting temperature (T_m), glass transition temperature (T_g), crystallization temperature (T_c), heat of fusion (ΔH_f), and the degree of crystallinity (X_c) are summarized in Table II. The T_m of 70PET/30PC/2HNTs was significantly higher with the presence of

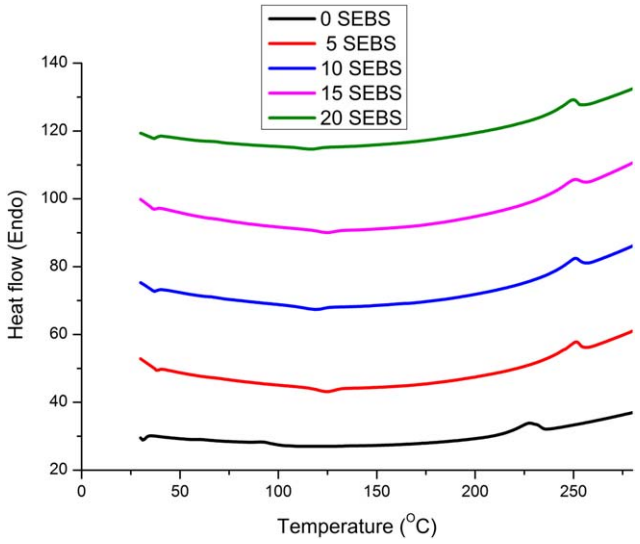

Figure 7. DSC heating scans of PET/PC/HNTs nanocomposites. [Color figure can be viewed in the online issue, which is available at wileyonlinelibrary.com.]

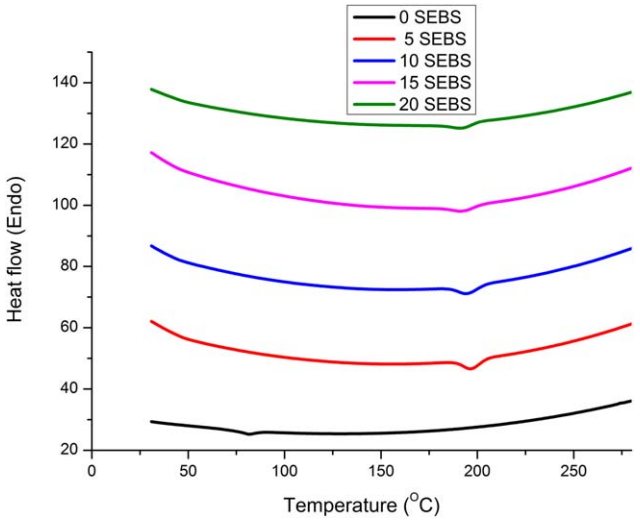

Figure 8. DSC cooling scans of PET/PC/HNTs nanocomposites. [Color figure can be viewed in the online issue, which is available at wileyonlinelibrary.com.]

SEBS-*g*-MA. This indicates that the addition of SEBS-*g*-MA influence the phase structure of nanocomposites. Kusmono *et al.*[22] have reported similar observation that addition of SEBS-*g*-MA increased T_m of PA6/PP/OMMT which suggests that phase a transformation occurred.

Notably a single T_g was observed for compatibilized nanocomposites which is higher than SEBS0 nanocomposites. The increased T_g is attributed to the higher T_g of PC. This is attributed to the good interfacial contact between PET and PC phases with incorporation of SEBS-*g*-MA. This is also consistent with the report by Ma *et al.*[23] on effects of compatibilizer on PET/PC blends. Single T_g indicates that the compatibility between the components has improved and became homogenous.

It can be seen that, the addition of SEBS-*g*-MA increased the crystallization temperature of 70PET/30PC/2HNTs nanocomposites. The T_c values of SEBS0 nanocomposites increased by around 115°C with the incorporation of 5 phr SEBS-*g*-MA. Beside, the increase in crystallization temperature, the X_c has also been improved with the addition of SEBS-*g*-MA. It has been shown that well dispersed HNTs act as nucleation agent leading to increase in crystallization rate and crystallinity of semi crystalline polymers.[24] This behavior is akin to other inorganic nanoparticle such as MMT and carbon nanotubes. It can be

Table II. Thermal Characteristic of PET/PC/HNTs/SEBS-*g*-MA Nanocomposites

Samples	T_m (°C)	T_{g1} (°C)	T_{g2} (°C)	T_c (°C)	ΔH_f (J/g)	X_c
SEBS0	227.3	58.4	95.7	81.6	17.7	21.0
SEBS5	251.1	-	127.7	196.6	21.1	25.1
SEBS10	251.2	-	124.9	194.8	20.1	23.9
SEBS15	250.0	-	128.0	192.3	18.1	21.5
SEBS20	249.3	-	124.7	192.0	18.0	21.4

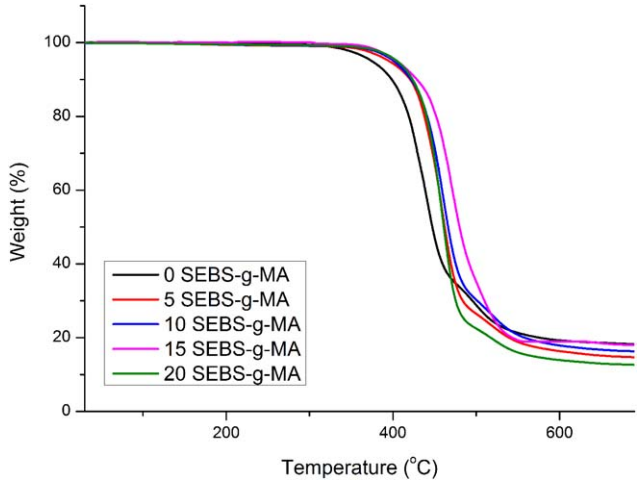

Figure 9. TGA curves of PET/PC/HNTs/SEBS-*g*-MA nanocomposites. [Color figure can be viewed in the online issue, which is available at wileyonlinelibrary.com.]

concluded that the addition of SEBS-*g*-MA improved the dispersion of HNT, and that well dispersed HNT results in the increase in crystallization rate and crystallinity of the blend matrix due to nucleation effect. Both of these observations are attributed to the better dispersion of HNTs in the PET/PC/HNTs/SEBS-*g*-MA nanocomposites. A Similar observation was reported by Kusmono *et al.*[22] on PA6/PP/OMMT/SEBS-*g*-MA nanocomposites. They found that the incorporation SEBS-*g*-MA into PA6/PP/MMT increased the degree of crystallinity due to the better dispersion and the formation of exfoliated structure in the nanocomposites.

Thermogravimetric Analysis. The thermogravimetric analysis (TGA) and derivative thermograms (DTG) for the PET/PC/HNTs/SEBS-*g*-MA nanocomposites are shown in Figures 9 and 10. The details are summarized in Table III. The initial decomposition temperature indicated by the 10% weight loss for SEBS0 was 397.3°C and temperature for maximum rate of decomposition was 441.4°C. It can be seen that the addition of SEBS-*g*-MA increased the thermal stability of the nanocomposites. As shown in Table III, the SEBS15 nanocomposites were most thermally stable. At that composition, both the initial decomposition temperature and maximum rate of decomposition temperature were higher than SEBS0 nanocomposites. However the char residue for SEBS15 did not improve compared to SEBS0 nanocomposites. The increased of thermal stability could be attributed to the interaction between MA group of SEBS-*g*-MA with the hydroxyl end group of PET and PC. Kusmono *et al.*[17] have reported similar observation that addition of SEBS-*g*-MA improved the thermal stability of PA6/PP. They found that the increased thermal stability was due to the SEBS-*g*-MA which act as compatibilizer leading to the improved interfacial adhesion between the phases.

However, further addition of SEBS-*g*-MA to 20 phr led to a decrease in thermal stability of the nanocomposites. Temperature at 10% weight loss and temperature at maximum rate of decomposition declined from 428.1 to 423.3°C and 442.3 to 441.0°C, respectively, as the SEBS-*g*-MA content increased from 15 to 20 phr contents. This result indicates that 15 phr is the optimum amount of SEBS-*g*-MA that can be added into the PET/PC/HNTs nanocomposites. In a related study, Inuwa *et al.*[25] observed that 10 phr SEBS-*g*-MA is the optimum concentration for the effective compatibilization of PET/PP in PET/PP/GNP nanocomposites. Similarly, Chow and Neoh[20] reported on effect of SEBS-*g*-MA on PC/MMT nanocomposites. They observed that the thermal stability decreased with high content of SEBS-*g*-MA due to the excess amount of SEBS-*g*-MA. According to Tjong and Bao,[26] the MA group grafted with SEBS may be degraded into –COOH at temperature around 200°C.

Scanning Electron Microscopy. Figure 11 shows the SEM micrographs of tensile fracture surface of 70PET/30PC/2HNTs nanocomposites with and without SEBS-*g*-MA. It can be seen that the SEBS0 nanocomposites surface containing pull out cavities and coalescence of PC aggregates. This indicates that poor interfacial adhesion between the PET and PC which results in the brittle failure of nanocomposites. On the contrary, the presence of 5 phr of SEBS-*g*-MA produced uniform and homogenous morphology [Figure 11(b)]. The addition of SEBS-*g*-MA improved interfacial adhesion between the phases. This could be attributed to the compatibilization effect of SEBS-*g*-MA. The compatibility of the polymers will be improved by maleic anhydride grafted elastomer, because the functional group (–MA) reacts with end group (–OH) of PET and PC, which strengthen interfacial adhesion and improve the compatibility between components.[16] The homogeneous and fibrillar morphology were observed with incorporation of 10 and 20 phr SEBS-*g*-MA [Figure 11(c,d)]. It can be seen that, a transition from a brittle type to ductile of morphology was observed with increased SEBS-*g*-MA. Similar observation was reported by Kusmono *et al.*[17] on effect of SEBS-*g*-MA on PA6/PP nanocomposites. They reported that extensive fibrillation morphology observed indicates that a good ductility and resistance to a crack propagation.

Transmission Electron Microscopy. The TEM images of SEBS0 and SEBS5 nanocomposites are shown in Figure 12 respectively. As can be seen from Figure 12(a), the agglomeration of the HNTs can be clearly observed in the uncompatibilized

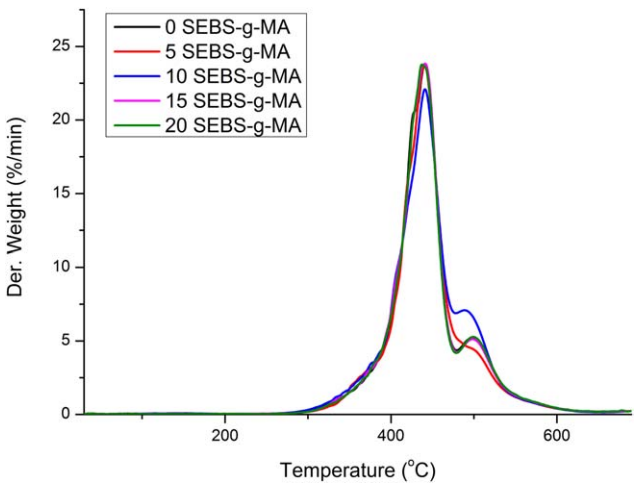

Figure 10. DTG curves of PET/PC/HNTs/SEBS-*g*-MA nanocomposites. [Color figure can be viewed in the online issue, which is available at wileyonlinelibrary.com.]

Table III. The Thermal Stability of PET/PC/HNTs/SEBS-*g*-MA Nanocomposites

Samples	Temperature at 10% weight loss (°C)	Temparature at maximum rate of weight loss (°C)	Residue at 650°C (%)
SEBS0	397.3	441.4	18.6
SEBS5	421.3	441.6	15.1
SEBS10	421.7	442.0	16.7
SEBS15	428.1	442.3	18.5
SEBS20	423.3	441.0	13.0

nanocomposites. Prashanta *et al.*[27] reported a similar observation for PP/HNTs nanocomposites. The existence of agglomerates indicates that insufficient interaction between HNTs and the matrix. It can be seen that the dispersion of the HNTs inside the matrix was improved with incorporation of 5 phr SEBS-*g*-MA [Figure 12(b)]. The HNTs are uniformly distributed and dispersed homogeneously. The improved dispersion of HNTs in the matrix was due to the introduction of hydrogen bonding which further improved the interface between fillers and matrix. In a study of PP/MMT nanocomposites reported by Chow and Neoh,[20] the preference of silicate layers to be dispersed at the edge of the SEBS-*g*-MA indicates that the polar MA functional groups grafted to the SEBS would rather interact with the hydroxyl groups of the clay present at the edge surface. In this case it is proposed that HNTs prefer to interact with the polar SEBS-*g*-MA due to the formation of hydrogen bonding between Si-O and Al-OH group of HNTs and OH groups of SEBS-*g*-MA. While the mechanism of the interaction between the anhydride groups of SEBS-*g*-MA with hydroxyl groups of PET (Figure 13)[16] and with PC (Figure 14)[28] have been well documented, a proposed scheme of interaction between MA, Si-OH and Al-OH is presented in Figure 15.

Fourier Transform Infrared Spectroscopy. Figure 16 shows the FTIR spectra of SEBS-*g*-MA, SEBS0 and SEBS5 nanocomposites. SEBS-*g*-MA showed an absorption peak at 2921 cm^{-1} which is assigned to the C–H stretching as reported by Alamri and Low.[29] The peak of absorption at 1630 cm^{-1}which correspond to the stretching of the carbonyl of MA in SEBS.[30] The new peak that appeared at 2926 cm^{-1} for SEBS5 can be attributed to the presence of SEBS-*g*-MA.[14] This indicates that the existence of hydrogen bonding within the molecular chain. The peak at 1012 cm^{-1} in the SEBS0 is assigned to the Si–O stretching.[29] This peak has shifted to 1015 cm^{-1} with incorporation of 5 phr SEBS-*g*-MA. The shifts of FTIR absorption peak is resulted from the formation of hydrogen bonds between the oxygen atoms of Si-O bonds on the surfaces of HNTs with SEBS-*g*-MA. Similar observations were reported by Pasbakhsh *et al.*[31] on HNTs/MAH-*g*-EPDM. They found that the shifting of Si-O stretching band was due the formation of hydrogen bonding between outer and inner surfaces of the HNTs with MAH-*g*-EPDM.

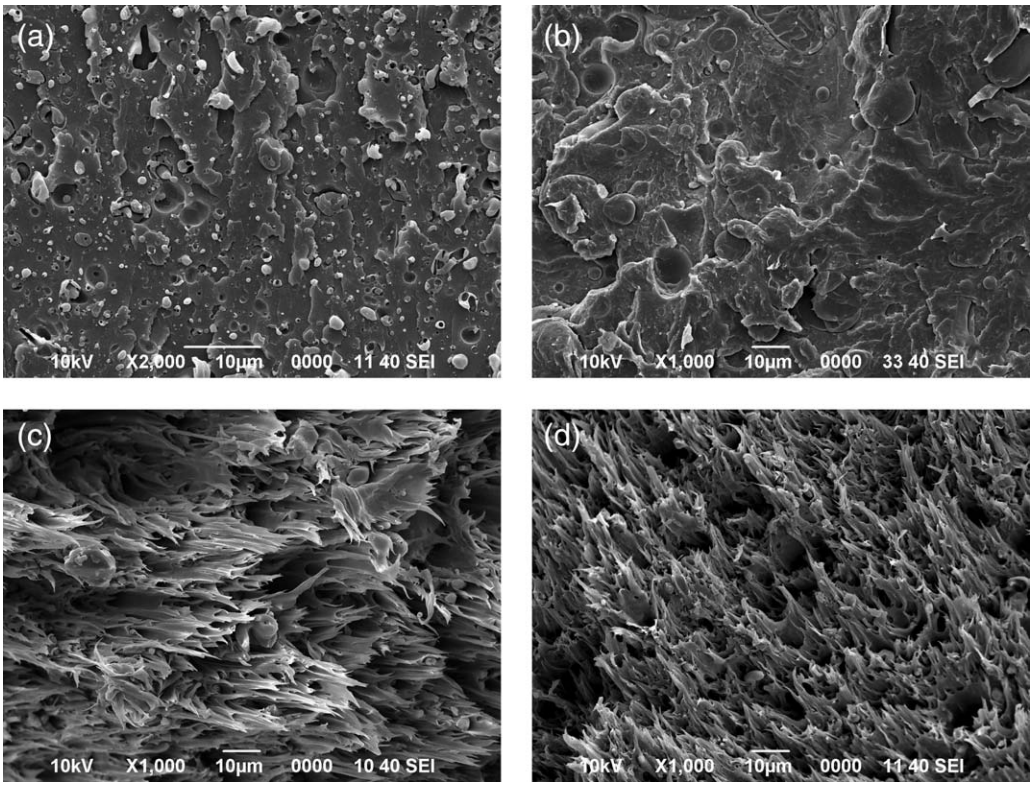

Figure 11. (a) SEM images of tensile fractured surfaces SEBS0. (b) SEM images of tensile fractured surfaces SEBS5. (c) SEM images of tensile fractured surfaces SEBS10. (d) SEM images of tensile fractured surfaces SEBS20.

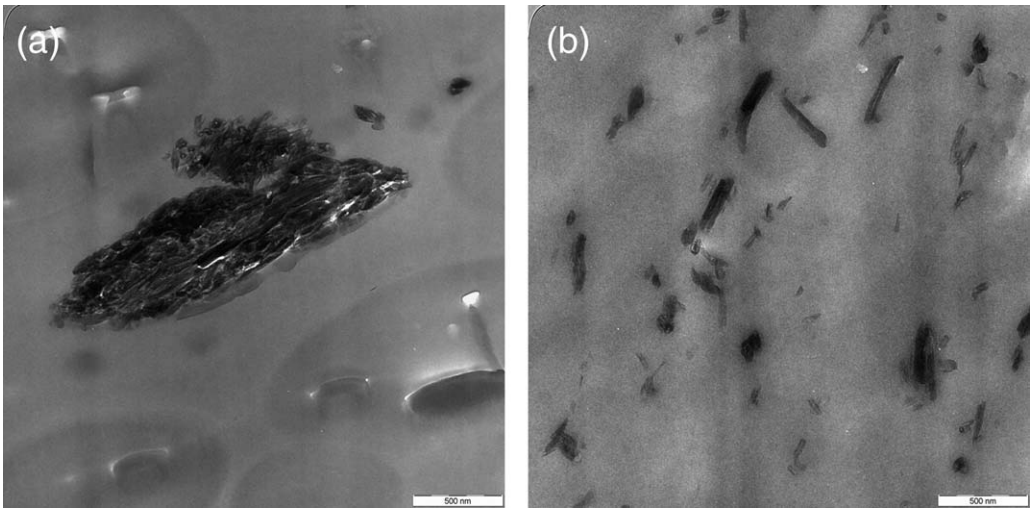

Figure 12. (a) TEM images SEBS0 nanocomposites. (b) TEM images SEBS5 nanocomposites.

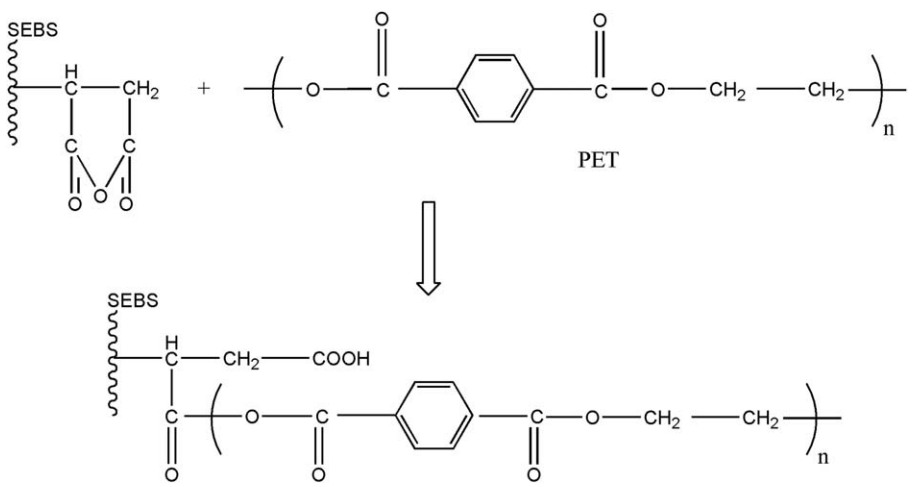

Figure 13. Interaction between SEBS-*g*-MA and PET.

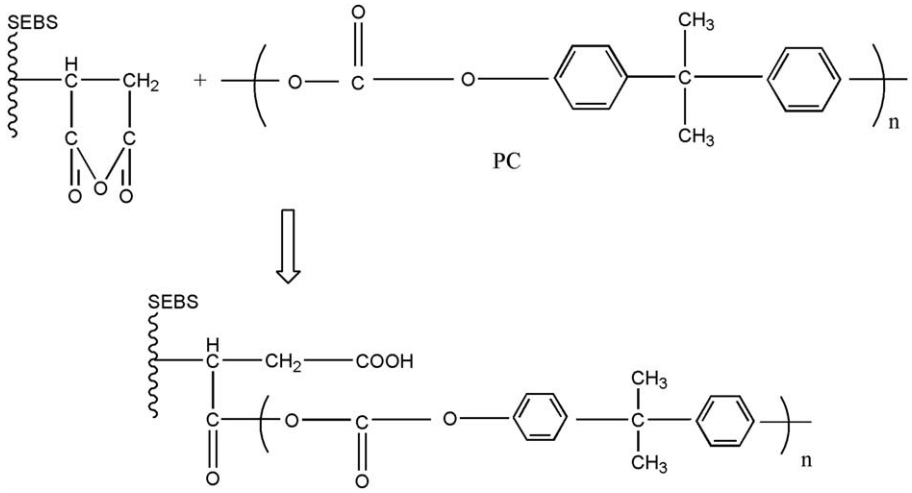

Figure 14. Interaction between SEBS-*g*-MA and PC.

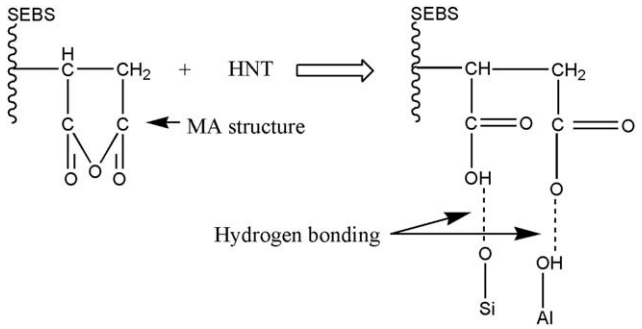

Figure 15. Proposed interactions between SEBS-*g*-MA and HNTs.

The peak at 2971 in the SEBS0 is attributed to the C–H strecthing of PET and PC.[14,32] The peak at 3621 cm^{-1} in the SEBS0 is assigned to OH stretching of HNTs.[29] The peaks at 3432 and 3545 cm^{-1} correspond to the O-H stretching for PET and PC.[6] It can be seen that the corresponding peaks are shifted to 3624, 3437, and 3546 cm^{-1} with incorporation of SEBS-*g*-MA. These shifts of absorption peaks resulted from the formation of hydrogen bonds between the anhydride group of SEBS-*g*-MA and hydroxyl groups of HNTs, PET, and PC.

CONCLUSIONS

This study revealed that the tensile and flexural strength of 70PET/30PC/2HNT were generally improved with incorporation of SEBS-*g*-MA with maximum values recorded at 5 phr. However, the tensile and flexural modulus of 70PET/30PC/2HNT nanocomposites were found to decrease with increasing of SEBS-*g*-MA content. The maximum improvement in impact strength (245%) was observed at 10 phr SEBS-*g*-MA. The elongation at break increased as the percentage of SEBS-*g*-MA increased. A single T_g was observed for compatibilized nanocomposites and it was higher than the T_g of SEBS0 nanocomposites due to the improved interfacial adhesion between the phases and a better dispersion of HNTs in the polymer matrix.

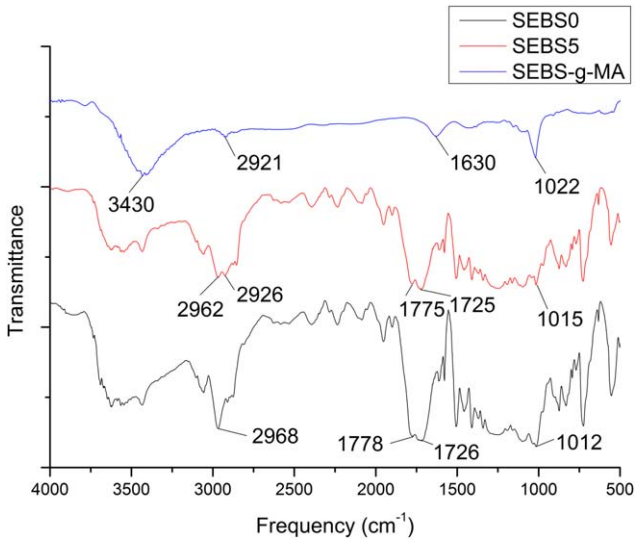

Figure 16. FTIR spectra of PET/PC/HNTs/SEBS-*g*-MA nanocomposites. [Color figure can be viewed in the online issue, which is available at wileyonlinelibrary.com.]

The thermal stability of 70PET/30PC/2HNTs nanocomposites was highest for the samples containing 15 phr SEBS-*g*-MA. SEM revealed a transition from a brittle to ductile morphology when 10 phr of SEBS-*g*-MA was added. TEM shows that HNTs are distributed and dispersed homogeneously with incorporation of SEBS-*g*-MA. The improvement in the properties of PET/PC/HNT/SEBS-*g*-MA was attributed to the improved interfacial adhesion between all phases resulting from the interaction via hydrogen bonding between SEBS-*g*-MA, PET, PC, and HNTs in the nanocomposites. FTIR analysis indicated such interactions. The developed compatibilized HNTs reinforced PET/PC nanocomposites have potential applications in the automotive industries where thermal stability with balanced stiffness, strength and toughness are required.

ACKNOWLEDGMENTS

The authors thank Universiti Teknologi Malaysia (UTM), Ministry of Higher Education Malaysia (MOHE), and Research University Grant Q.J130000.2509.05H22 for financial support.

REFERENCES

1. Baliga, S.; Wong, W. T. *J. Polym. Sci: Part A: Polym. Chem.* **1989**, *27*, 2071.
2. Shukla, S. K.; Kulkarni, K. S. *J. Appl. Polym. Sci.* **2002**, *85*, 1765.
3. Oromiehie, A.; Mamizadeh, A. *Polym. Int.* **2004**, *53*, 728.
4. Nassar, T. R.; Paul, D. R.; Barlow, J. W. *J. Appl. Polym. Sci.* **1979**, *23*, 85.
5. Murff, S. R.; Barlow, J. W.; Paul, D. R. *J. Appl. Polym. Sci.* **1984**, *29*, 3231.
6. Suzuki, T.; Tanaka, H.; Nishi, T. *Polymer* **1989**, *30*, 1287.
7. Kong, Y.; Hay, J. N. *Polymer* **2002**, *43*, 1805.
8. Kamble, R.; Ghag, M.; Gaikawad, S.; Panda, B. K. *J. Adv. Sci. Res.* **2012**, *3*, 25.
9. Du, M.; Guo, B.; Jia, D. *Eur. Polym. J.* **2006**, *42*, 1362.
10. Höchstotter, K. H.; Lim, G. T.; Altstädt, V. *Compos. Sci. Technol.* **2009**, *69*, 330.
11. Mubarak, Y. A. *Polym. Plast. Technol. Eng.* **2011**, *50*, 635.
12. Calcagno, C. I. W.; Mariani, C. M.; Teixeira, S. R.; Mauler, R. S. *Compos. Sci. Technol.* **2008**, *68*, 2193.
13. Lim, S. R.; Chow, W. S. *J. Appl. Polym. Sci.* **2012**, *123*, 3173.
14. Tanrattanakul, V.; Hiltner, A.; Baer, E. *Polymer* **1997**, *38*, 2191.
15. Chiu, H. T.; Hsiao, Y. K. *J. Polym. Res.* **2006**, *13*, 153.
16. Tang, X.; Guo, W.; Yin, G.; Li, B.; Wu, C. *Polym. Bull.* **2007**, *58*, 479.
17. Kusmono; Mohd Ishak, Z. A.; Chow, W. S.; Takeichi, T.; Rochmadi *Eur. Polym. J.* **2008**, *44*, 1023.
18. Zhang, Y.; Zhang, H.; Ni, L.; Zhou, Q.; Guo, W.; Wu, C. *J. Polym. Environ.* **2010**, *18*, 647.
19. Tjong, S. C.; Bao, S. P. *J. Polym. Sci. Part B: Polym. Phys.* **2005**, *43*, 585.

20. Chow, W. S.; Neoh, S. S. *Polym. Plast. Technol. Eng.* **2010**, *49*, 62.
21. Heino, M.; Kirjava, J.; Hietaoja, P.; Seppala, J. *J. Appl. Polym. Sci.* **1997**, *65*, 241.
22. Kusmono; Mohd Ishak, Z. A.; Chow, W. S.; Takeichi, T. *Compos. Part A: Appl. Sci. Manuf.* **2008**, *39*, 1802.
23. Ma, D.; Zhang, G.; He, Y.; Ma, J.; Luo, X. *J. Polym. Sci. Part B: Polym. Phys.* **1999**, *37*, 2960.
24. Du, M.; Guo, B.; Jia, D. *Polym. Int.* **2010**, *59*, 574.
25. Inuwa, I. M.; Hassan, A.; Samsudin, S. A.; Haafiz, M. K. M.; Jawaid, M.; Majeed, K.; Razak, N. C. A. *J. Appl. Polym. Sci.* **2014**, *131*, 1.
26. Tjong, S. C.; Bao, S. P. *Compos. Sci. Technol.* **2007**, *67*, 314.
27. Prashantha, K.; Lacrampe, M. F.; Krawczak, P. *Exp. Polym. Lett.* **2011**, *5*, 295.
28. Yu, Z.; Yang, M. S.; Dai, S. C.; Mai, Y. W. *J. Appl. Polym. Sci.* **2004**, *93*, 1642.
29. Alamri, H.; Low, I. M. *Mater. Des.* **2012**, *42*, 214.
30. Socrates, G. **2004**. Infrared and Raman characteristic group frequencies: tables and charts. John Wiley & Son p 130.
31. Pasbakhsh, P.; Ismail, H.; Fauzi, M. N.; Bakar, A. A. *Polym. Test.* **2009**, *28*, 548.
32. Kraus, R. G.; Emmons, E. D.; Thompson, J. S.; Covington, A. M. *J. Polym. Sci.: Part B: Polym. Phys.* **2008**, *46*, 734.